# Energy-Efficient HVAC Systems: Simulation-Empirical Modelling and Gradient Optimization

V. Vakiloroaya[a], Q. P. Ha[a,]* and B. Samali[b]

[a]*School of Electrical, Mechanical and Mechatronic Systems,*
*University of Technology Sydney, Australia*

[b] *School of Civil and Environmental Engineering,*
*University of Technology Sydney, Australia*

## Abstract

This paper addresses the energy saving problem of air-cooled central cooling plant systems using the model-based gradient projection optimization method. Theoretical-empirical system models including mechanistic relations between components are developed for operating variables of the system. Experimental data are collected to model an actual air-cooled mini chiller equipped with a ducted fan-coil unit of an office building located in hot and dry climate conditions. Both inputs and outputs are known and measured from field monitoring in one summer month. The development and algorithm resulting from the gradient projection, implemented on a transient simulation software package, are incorporated to solve the minimization problem of energy consumption and predict the system's optimal set-points under transient conditions. The chilled water temperature, supply air temperature and refrigerant mass flow rate are calculated based on the cooling load and ambient dry-bulb temperature profiles by using the proposed approach. The integrated simulation tool is validated by using a wide range of experimentally-collected data from the chiller in operation. Simulation results are provided to show possibility of significant energy savings and comfort enhancement using the proposed strategy.

**Keywords:**

Central Cooling Plant; Experimental Study; Gradient Projection Method; Energy Savings; Comfort

________

* *Corresponding author. E-mail: Quang.Ha@uts.edu.au*,
Postal Address: PO Box 123, Broadway, Sydney, NSW, 2007, Australia

## Nomenclature

| | |
|---|---|
| $A$ | orifice area (m$^2$) |
| $AU$ | overall heat transfer coefficient of evaporator (kW/°C) |
| $C$ | mass flow coefficient |
| $C_p$ | constant pressure specific heat (kJ/(kg °C)) |
| $d_i$ | expansion valve inlet diameter (m) |
| $D$ | orifice diameter (m) |
| $k$ | compression index |
| $l$ | cooling coil length (m) |
| $LMTD$ | logarithmic mean temperature difference (°C) |
| $M_{ccw}$ | cooling coil water mass (kg) |
| $\dot{m}$ | mass flow rate (kg/s) |
| $n$ | compressor speed (rad/s) |
| $P_{cf}$ | variable air volume fan power consumption of the condenser (kW) |
| $P_{comp}$ | compressor power consumption (kW) |
| $p_{dis}$ | discharge pressure (kPa) |
| $P_{fcu}$ | variable air volume fan power consumption of the ducted fan-coil unit (kW) |
| $p_i$ | upstream pressure of the expansion valve (kPa) |
| $p_o$ | downstream pressure of the expansion valve (kPa) |
| $p_{suc}$ | suction pressure (kPa) |
| $P_{total}$ | total power consumption of central cooling plant (kW) |
| $Q$ | heat capacity (kW) |
| $Q_b$ | building cooling load (kW) |
| $r$ | radius of the rotor (m) |
| $s_c$ | stork of the cylinder (m) |
| $T$ | temperature (°C) |
| $v$ | velocity (m/s) |
| $\dot{V}_{comp}$ | refrigerant flow rate of the compressor (m$^3$/s) |
| $\dot{V}_{con}$ | air-cooled condenser air flow rate (m$^3$/s) |
| $\dot{V}_{\mathrm{sup}}$ | Cooling coil air volume (m$^3$) |
| $w_{comp}$ | indicated work input to compressor (kJ/kg) |
| $w_{comp,t}$ | isentropic work input to compressor (kJ/kg) |
| $\phi$ | overall displacement coefficient of the compressor |
| $\varepsilon$ | relative eccentricity of the rotor |
| $\mu_r$ | refrigerant dynamic viscosity (Pa.s) |
| $\rho$ | density (kg/m$^3$) |
| $\sigma_i$ | surface tension (N/m) |
| $\eta_{comp}$ | total efficiency of the compressor |

### Subscripts

| | |
|---|---|
| $a$ | air |
| $cc$ | cooling coil |
| $chw$ | chilled-water |
| $con$ | condenser, condensing |
| $db$ | dry-bulb |
| $eva$ | evaporator, evaporative |
| $i$ | inlet |
| $o$ | outlet |
| $r$ | refrigerant |
| $ret$ | return |
| $sup$ | supply |
| $w$ | water |

## 1. Introduction

As the energy needs of the world are growing with the increasing population, researchers have made great efforts to lead to energy-efficient processes and preserve the environment. About half of the total energy consumption of our modern society is consumed in buildings, in which a major proportion is for Heating, Ventilating and Air-Conditioning (HVAC). Therefore, much research has focused on energy savings in HVAC systems. Among their several types, the air-cooled chillers are responsible for 60% of the electricity used for air-conditioning which can amount to 25-40% of the total electricity consumption of an air-conditioned building [1]. Furthermore, air-cooled chillers together with their air handling units remain a popular choice for industrial and commercial air conditioning due to their easy installation, simplicity of operation and lower maintenance costs compared to water-cooled chillers. Therefore, energy efficiency improvements for these chillers can significantly reduce buildings' power consumption.

The field of energy control of central cooling plants to enhance system performance and efficiency has recently attracted much research attention [2-5]. Apart from efforts devoted to the development of eco-friendly and energy-efficient HVAC technologies using renewable energy sources such as solar energy [6-8], several studies have highlighted the potential impact of optimisation on energy and comfort of HVAC systems. Congradac and Kulic [9] described the use of genetic algorithms for optimal operation of HVAC systems. A simulation was conducted to demonstrate how much power can be saved via the suggested method. Wemhoff [10] applied a novel control method using multi-dimensional interpolation of optimised control configurations for various load distributions. The results showed the method was able to save energy by 19% as compared to an uncontrolled system. Zaheeruddin and Ning [11] developed a neural network based optimization algorithm to find the optimal set-points for a variable air volume HVAC system. Their results showed that an optimal operation strategy could offer a remarkable energy savings under partial load conditions. Ma and Wang [12] presented a model-based supervisory and optimal control strategy for central chiller plants to enhance the system performance and energy efficiency with 0.73-2.25% of daily energy savings via a reference using traditional settings. Recently, Beghi and Cecchinato [13] have designed an adaptive controller for a packaged air-cooled water chiller, using the quasi steady-state and a moving boundary model for the chiller dynamics to evaluate the effect of energy losses during the system operation time. Their algorithm could grant 3-7.3% improvement in energy savings with respect to supply water temperature control. All these studies primarily demonstrated their energy saving potential in HVAC systems associated with the use of control techniques. On the other hand, operational optimization of HVAC system components taking into account human comfort has attracted less attention while it represents directly investments required to ensure that the system installed in buildings are operating in an optimal mode. More importantly, reports on practical optimal control strategies for chilled water systems seem to be still sparse in the literature.

The objective of this research is to obtain valid models for operational components of central cooling plant HVAC systems, to develop an optimal strategy for their control variables for minimizing the energy consumption while satisfying comfort conditions, and to evaluate the implementation of the developed algorithm on a real-world office building. Here, a physical-empirical approach is used to obtain the system models, from which the proposed optimal control strategy is formulated. The system's control variables are continuously updated online by using the gradient projection method to search for global and local minima. A numerical algorithm is then developed to obtain optimal settings from the minimization of an objective function. Furthermore, energy efficiency and performance of the proposed strategy are verified and evaluated with data collected from an actual air-cooled chiller, installed in a building as a case study. In order to quantify and determine optimal control variables of the cooling plant, several field tests were conducted. A linear constraint, formulated by using experimentally-collected data and empirically-based regression, is incorporated to impose the required range limits for the control variables. To deal with complexity of the heat transfer process, building-dependency of the HVAC system, and the increased cumbersome computation, a transient simulation software package [14], is used to predict the HVAC system performance under optimizing control variable set-points in the presence of transient loads. The cooling plant models, experimental data and proposed optimization algorithm are coded and implemented within the TRNSYS-16 environment so that dynamic predictions of all main equipment in the whole system can be performed simultaneously. To show effectiveness of the proposed control strategy, a predicted mean vote (PMV) index is computed for the building under investigation. The results obtained show a significant energy saving potential when using the proposed approach while maintaining the building indoor comfort conditions. As of a generic nature, this optimization technique can be applied to any central cooling plant.

The paper is organized as follows. After the introduction, Section 2 describes the mathematical models using the proposed simulation-empirical modelling approach. Section 3 presents the formulation of the gradient projection method of the HVAC system together with its optimization algorithm. The set-up and uncertainty analysis are described in Section 4. The results and discussion are included in Section 5. Finally, a conclusion is drawn in Section 6.

## 2. Mathematical Models

The schematic of the central cooling plant is shown in Fig. 1(a) while the log pressure-enthalpy (p-h) diagram for the air-cooled chiller using the R134a refrigerant in steady-state conditions is shown in Fig. 1(b). The system comprises an air-cooled scroll chiller, a ducted fan-coil as the air-handling unit, chilled water pumps, valves and connection tubes. Efficiency of vapour compression chillers depends strongly on the system variable set-points. Furthermore, nonlinearity and complexity inherently existing in the dynamic process of a central cooling plant make it difficult to be represented accurately by using only thermodynamic and heat transfer models. Fortunately, these models can be developed empirically from the experimental monitored data for application in optimal operations of the system in consideration. Adopting the method reported in [15], this section presents the physical-empirical models for the system components by using real-world data experimentally collected. These models then are implemented in the simulation tool TRNSYS-16 to extract the right system dynamics and examine the optimization approach, taking the advantage of the versatile software, wherein heat transfer and thermodynamic laws are incorporated for reliable transient analysis.

### 2.1. Air-Cooled Chiller

Many models for chillers have been developed using various principles, see [16-18]. To target the system's energy efficiency, our objective is to predict the air-cooled scroll chiller's power consumption in relation to the supply chilled water temperature and the refrigerant mass flow rate, while its thermodynamic transient performance is analysed by using TRNSYS. A regression function is used to describe the relationship of the power consumption and these controlled variables. The chiller comprises a variable speed rotary compressor, an air-cooled condenser, an electronic expansion valve (EEV) and a direct expansion (DX) evaporator. A combined theoretical-empirical modelling approach is developed herein to allow for performance prediction over a very wide range of operating conditions.

#### 2.1.1. Direct Expansion Evaporator

The DX evaporator in the plant is a heat exchanger of the shell and tube flooded type. The cooling capacity of the evaporator $Q_{eva}$ is expressed as the product of the overall heat transfer coefficient and the logarithmic mean temperature difference (LMTD) of the evaporator:

$$Q_{eva} = (AU)_{eva} LMTD_{eva}, \tag{1}$$

$$(AU)_{eva} = \frac{1}{a_0(\dot{m}_{chw})^{a_1} + a_2(Q_{eva})^{a_3} + a_4}, \tag{2}$$

$$LMTD_{eva} = \frac{(T_{chw,i} - T_{eva}) - (T_{chw,o} - T_{eva})}{\ln \dfrac{T_{chw,i} - T_{eva}}{T_{chw,o} - T_{eva}}}, \tag{3}$$

where coefficients $a_0$ to $a_4$ are constant to be estimated based on the collected performance data of the chiller.

#### 2.1.2. Variable Speed Rotary Compressor

In this study a steady-state polytropic compression is considered, assuming the compressor's speed reaches its specified speed instantaneously. In the variable speed rotary compressor, the speed can be continuously varied to modulate the required cooling capacity for the evaporator. The inlet and outlet compressor refrigerant flow rates are assumed to be equal, i.e.

$$\dot{m}_{r,i} = \dot{m}_{r,o} = \rho_r \dot{V}_{comp}, \tag{4}$$

where its refrigerant flow rate is given by:

$$\dot{V}_{comp} = n\pi r^2 s_c \varepsilon(2-\varepsilon)\phi. \tag{5}$$

The theoretical isentropic work of the compressor can be calculated by:

$$w_{comp,t} = \left(\frac{k}{k-1}\right)\left(\frac{p_{suc}}{\rho_r}\right)\left(\left(\frac{p_{dis}}{p_{suc}}\right)^{\frac{k-1}{k}} - 1\right). \tag{6}$$

In this study the compression index $k$ takes the value of 1.1 for R-134a refrigerant. The indicated work of the compressor can then be determined by:

$$w_{comp} = \frac{w_{comp,t}}{\eta_{comp}}, \tag{7}$$

where $\eta_{comp}$ is the total efficiency of the compressor. The empirical expression to determine the power consumption of the compressor $P_{comp}$ is proposed as follows:

$$\begin{aligned} P_{comp} = {} & b_0 + b_1 T_{chw,o} + b_2 T_{chw,o}^2 + b_3 T_{chw,o} Q_b + b_4 T_{chw,o} \dot{m}_r + b_5 T_{chw,o}^2 Q_b + b_6 T_{chw,o}^2 \dot{m}_r \\ & + b_7 T_{chw,o} Q_b^2 + b_8 T_{chw,o} \dot{m}_r^2 + b_9 \dot{m}_r Q_b, \end{aligned} \tag{8}$$

where the ten coefficients $b_0$ to $b_9$ are constant to be determined by curve-fitting of the experimentally-collected data.

### 2.1.3 Electronic Expansion Valve (EEV)

The expansion valve is a refrigerant flow control device that adjusts the quantity of the liquid refrigerant entering the evaporator, and thus regulates the refrigerant superheat temperature leaving the evaporator. The most effective variable for optimal operation of EEV is the refrigerant mass flow rate while the cooling load is considered as uncertain [19]. The refrigerant flow through the EEV is represented by the orifice equation for calculation of its mass flow rate:

$$\dot{m}_r = C\left(\frac{\pi D^2}{4}\right)\sqrt{2\rho_r(p_i - p_o)}, \tag{9}$$

where the mass flow coefficient $C$ is a function of the valve's geometric parameters, the inlet refrigerant pressure and temperature, the outlet refrigerant pressure, and the refrigerant thermo-physical properties [20]:

$$C = 1.1868 \times 10^{-13} \left( \frac{(p_i - p_o)\sqrt{A}}{\sigma_i} \right)^{-1.4347} \left( \frac{d_i \sqrt{\rho_r p_i}}{\mu_r} \right)^{3.6426}. \tag{10}$$

#### 2.1.4. Air-Cooled Condenser

The condenser model is derived from the heat rejection of the condenser air, based on the energy balance. It can be expressed as the product of the condenser's overall heat transfer coefficient and its logarithmic mean temperature difference:

$$Q_{con} = (AU)_{con} LMTD_{con}, \tag{11}$$

$$(AU)_{con} = \frac{1}{a_5 (\dot{V}_{con})^{a_6} + a_7 (\dot{m}_r)^{a_8} + a_9}, \tag{12}$$

$$LMTD_{con} = \frac{(T_{con} - T_{db}) - (T_{con} - T_{con,a,o})}{\ln \dfrac{T_{con} - T_{db}}{T_{con} - T_{con,a,o}}}, \tag{13}$$

where constant parameters $a_5$ to $a_9$ are evaluated by curve-fitting the chiller performance data. The power consumption of the air-cooled condenser fan $P_{cf}$ is proposed as:

$$P_{cf} = c_0 + c_1 \dot{m}_r + c_2 \dot{m}_r^2 + c_3 \dot{m}_r T_{db} + c_4 \dot{m}_r^2 T_{db} + c_5 \dot{m}_r T_{db}^2, \tag{14}$$

where coefficients $c_0$ to $c_5$ are constant values to be determined again by curve-fitting.

### 2.2. Ducted Fan Coil Unit

The purpose of the fan-coil unit is to handle the supply air in buildings. The main parts of a fan-coil unit are the cooling coil and the supply fan. The heat transfer properties of the water cooling coil have direct influences on the performance of the air-cooled chiller [21]. By using the energy and mass conservation laws, the dynamic change of the air and water temperature through the cooling coil is described as [22]:

$$M_{cc,w}\left(C_{p,w}\frac{dT_{cc,w}}{dt}+C_{p,w}v_w\frac{T_{chw,o}-T_{chw,i}}{l}\right)=Q_{cc}, \tag{15}$$

$$\rho_a V_{\sup}\left(C_{p,a}\frac{dT_{\sup}}{dt}+C_{p,a}v_a\frac{T_{\sup}-T_{ret}}{l}\right)=-Q_{cc}, \tag{16}$$

The speed of supply fan can be controlled to improve the whole cooling coil's performance. In this study, a quadratic form for the ducted unit variable air volume fan is proposed, which represents the total power consumption in terms of the supply air temperature $T_{sup}$, chilled water temperature $T_{chw,o}$ and building cooling load $Q_b$:

$$\begin{aligned}P_{fcu} &= d_0+d_1T_{\sup}+d_2T_{\sup}^2+d_3T_{\sup}Q_b+d_4T_{\sup}T_{chw,o}+d_5T_{\sup}^2Q_b+d_6T_{\sup}^2T_{chw,o}\\ &+d_7T_{\sup}Q_b^2+d_8T_{\sup}T_{chw,o}^2+d_9T_{chw,o}Q_b,\end{aligned} \tag{17}$$

where coefficients $d_0$ to $d_9$ are constant values and can be determined by curve-fitting the real data.

## 3. Methodology

This section describes our proposed approach for power consumption minimization in the cooling system. The optimization problem is formulated through the determination of the controlled variables to achieve minimum of an objective function subject to constraints.

### 3.1. Gradient Projection Optimization

The gradient projection method is applied here to solve the optimization problem. This method is based on projecting the search direction into the subspace tangent to the active constraints. The basic assumption of the gradient projection method is that the independent variable vector lies in this subspace. The optimization problem with linear equality constraints is formulated as:

$$\begin{aligned}&\textit{Minimize}\ \ f(X)\\ &\textit{subject to}\ g(X)=N^TX-b=0,\end{aligned} \tag{18}$$

where $f(X)$ is the objective function to be minimized, $g(X)$ is an $m$-vector of active constraints, $X=(x_1,x_2,\ldots,x_n)^T$ is the vector of independent variables, $N$ is an $n\times m$-matrix $(n>m)$ whose columns are the gradient of constraints and $b$ is a constant $m$-vector.

The basis of the gradient projection method is to find an $n$-dimensional vector $s$, which is projected according to the steepest descent direction onto the constraint gradient. Therefore, the constrained optimization (18) using the gradient projection method is cast as:

$$\begin{aligned} &Minimize\ s^T \nabla f, \\ &subject\ to\ N^T s = 0, \\ &and \quad s^T s = 1. \end{aligned} \tag{19}$$

Here, we apply the classical Lagrange subject to equality constraints to minimize the above function. Since vector $s$ defines the search direction, the unnormalized gradient projection vector $U(X)$ used for updating $X$ is as [23]:

$$U(X) = -P\nabla f, \tag{20}$$

where $P$ is the projection matrix defined as:

$$P = \left(I - N(N^T N)^{-1} N^T\right), \tag{21}$$

in which $I$ is the $n \times n$ identity matrix.

The minimum values of the objective function are achieved when $U(X)$=0, whereby a given small number can be deliberately chosen for a termination condition. The following iterative equation for updating $X$ is used:

$$X_{k+1} = X_k + \beta U_k, \tag{22}$$

where $\beta$ can be obtained from a one-dimensional search. This algorithm has been coded into a dedicated TRNSYS interface, GenOpt, using the TRNOPT module. Here, we have modified the TRNOPT with our proposed algorithm and couple it into the TRNSYS simulation program for optimization and implemented the algorithm into the library of available optimization codes. This program thus can read inputs files, call the simulation program TRNSYS and then write output files.

### 3.2 Optimization Algorithm

In this paper the objective is to minimize of the overall power consumption of the whole system with controlled variables being the refrigerant mass flow rate, chilled-water temperature and supply air temperature. The uncontrolled variables include the building cooling demand and ambient dry-bulb temperature. The total power consumption $P_{total}$ is the sum of the compressor power, fan-coil unit power and condenser fan power. Thus, the optimization problem here is stated as:

$$\begin{aligned} &Min\ \ P_{total} = P_{comp} + P_{fcu} + P_{cf} = f\left(\dot{m}_r, T_{\sup}, T_{chw,o}, Q_b, T_{db}\right), \\ &\text{subject to}\ \ \text{constraint}\ \ \mathscr{C} \end{aligned} \tag{23}$$

This constraint can be obtained by referring to the system models and by using the experimental data as follows:

$$\mathscr{C}:\ \ e_0 + e_1 T_{chw,o} + e_2 T_{\sup} + e_3 \dot{m}_r + e_4 Q_b + e_5 T_{db} = 0, \tag{24}$$

where coefficients $e_0$ to $e_5$ are constant parameters to be determined by curve-fitting the experimental data, taking into account the comfort range of the room temperature and humidity.

To begin the simulation, the program reads the first set of operating data, such as the evaporative and condensing pressure of the refrigerant, supply and return chilled-water temperature, chilled-water mass flow rate, refrigerant mass flow rate and air flow rate of the evaporator and condenser. The remaining system characteristics are then calculated by using the aforementioned mathematical models as well as monitored experimental data. The simulation algorithm continues until all system parameters are specified after having incorporated each component of the system. The chiller model includes also a subroutine to evaluate the thermodynamic properties of the refrigerant R-134a. In order to solve the optimization problem, a computational sub-algorithm is developed and implemented within the GenOpt program. The flow chart for that is shown in Fig. 2. Here, an iteration loop is proposed to find optimal set-points of the chilled water temperature, refrigerant mass flow rate and supply air temperature. These control variables are considered to vary correspondingly in restricted ranges as imposed by HVAC system operation requirements. Based on the gradient projection method, these operation variables are computed and kept in a storage file by using the proposed algorithm. These data are then compared with those obtained from the conventional central cooling plant to indicate the energy efficiency improvement of the proposed system.

### 3.3 Model Verification

The mathematical model and experimental data for the system components are implemented in TRNSYS based on a modular approach coded in the form of FORTRAN subroutines. The building information file created by PREBID, compliant with the requirements of the ANSI/ASHRAE Standard 140-2007 [24]. The simulation is run with a time interval of 15 minutes that is equal to the monitoring time step in the real test process of the cooling plant. Constant parameters of the component models are required to be verified. According to the data collected from the field tests, the corresponding coefficients of the models and constraints are obtained from regression techniques by using the MINITAB statistical software [25]. The R-squared value of each model indicates a good fit for its parameters. The regression process adjusts the coefficients in terms of variations in the actual overall system energy consumption. These coefficients obtained for the central cooling plant under investigation are shown in Table 1.

In order to verify the appropriateness of using the estimation values obtained by the simulation, it is important to validate the accuracy of the models under various operational conditions. To test the accuracy of the chiller model, a comparison is made between the predicted and actual values of the compressor electric demands over a two-week period during which the chiller was operated continuously from 8 a.m. to 6 p.m. The results are depicted in Fig. 3, where it can be seen that only 24% of the total predicted data deviate from the actual data by more than 5% and all modelled data have a prediction error of less than 10%.

## 4. Experimental Set-Up and Statistics

The proposed optimization process is applied on the existing mini air-cooled chiller and ducted fan-coil unit installed in an office building and used as our experimental set-up. The chiller includes an electronic expansion valve, a DX evaporator with copper tubes, an air-cooled condenser and a variable speed rotary compressor. Details of the system parameters and specifications are given in Table 2.

High precision sensors/transducers were used for measuring all operating variables. Manometers were used for measuring the condenser and supply air flow rate. The temperature sensor for the supply and return air is of platinum resistance type with accuracy ±0.1°C. The refrigerant mass flow rate passing through the EEV is measured by a Coriolis mass flow meter with accuracy ±1%. The ambient air temperature is monitored by a digital thermometer of precision ±0.8°C. Water temperatures are measured by mercury thermometers with precision ±0.2°C. Electric component powers are measured by a digital ac/dc power clamp multimeter of ±3.5% in precision. All measurement signals are acquired with a 15-minute sampling time. Therefore a total of 1440 points the system's power consumption and other variables were measured. Data were logged for the test system by using history sheets available in the system measuring tool. The building sensible and latent cooling loads corresponding to the dry-bulb temperature and the wet-bulb temperature of the building are calculated respectively from the monitoring data. Indoor sensible loads were determined by assuming that they are proportional to the product of the monitored supply fan air flow rate and the difference in the measured temperatures between the supply and return air zone while the building latent loads are proportional to the product of the fan air flow and the difference in the supply and return humidity ratios. Similarly, the evaporator capacity is determined by using the air flow rate of the evaporator and the difference between measured temperatures entering and leaving the air for sensible loads, or the difference between air humidity ratios for latent loads. These data are stored in TRNSYS by using separate external data files. The TRNSYS can interpolate and extrapolate these values during the simulation.

Experimental studies usually involve some unpredictable and uncertain factors which may occur due to instrumental manufacturing errors, calibration errors and human mistakes. These uncertainties should be excluded when evaluating the experimental results. For this, a statistical analysis is used for the experimentally-recorded data. The normalized deviation about the mean value is used for each reading $x_i$ from the following equation:

$$\varphi_i = \frac{x_i - x}{s_x}, \tag{25}$$

where the standard deviation $s_x$ is determined by:

$$s_x = \sqrt{\frac{1}{N}\sum_{i=1}^{N}(x_i - \bar{x})^2}, \tag{26}$$

and the average $\bar{x}$ is calculated from:

$$\bar{x} = \frac{1}{N}\sum_{i=1}^{N} x_i . \tag{27}$$

For each reading, the deviation (26) is compared with the ratio of the maximum allowable deviation from the mean value and standard deviation. Those values falling outside the allowable range will be removed from the recorded data. Consequently, a detailed error analysis indicates that the compressor power consumption determined by the proposed empirical method is subject to an overall tolerance of ±7.8%. Here, the overall uncertainty is found within ±6.3% and ±7.1% obtained respectively for the air-cooled condenser fan and the supply fan.

## 5. Results and Discussion

Having described the specifications of the plant and developed the strategy to obtain the optimal set-points for control variables, this section is devoted to the results and discussion on the electricity saving potential and thermal comfort ability as achieved from using the proposed optimization approach. TRNSYS is run to perform the system's component-wise energy analysis and obtain profiles of the indoor temperature and relative humidity throughout a summer. The cooling load is computed before running the simulation. The indoor temperature and relative humidity set-points for calculating the cooling load are respectively 23°C and 50%. The peak cooling load is estimated at 12.25 kW in the middle of July. The gradient projection-based optimizer starts with a trial using initially-guessed values of control variables at their default design conditions:

$$X_0 = \begin{bmatrix} T_{chw,o}^0 & T_{\sup}^0 & \dot{m}_r^0 \end{bmatrix}^T = \begin{bmatrix} 7 & 9 & 0.135 \end{bmatrix}^T . \tag{28}$$

The proposed algorithm then evaluates the projection matrix as:

$$P = \begin{bmatrix} 1.769 & -0.416 & 0.054 \\ -0.416 & 1.225 & -0.029 \\ 0.054 & -0.029 & 1.003 \end{bmatrix}. \tag{29}$$

The gradient vector of the objective function obtained at initial conditions is:

$$\nabla f(X_0) = \begin{bmatrix} 0.982 + 6.827Q_b \\ -0.213 + 0.013Q_b - 0.001Q_b^2 \\ -7.9 + 0.15Q_b + 0.6T_{db} - 0.006T_{db}^2 \end{bmatrix}. \tag{30}$$

The direction search at $X_0$ is therefore given by:

$$U_0 = -P\nabla f(X_0) = \begin{bmatrix} 1.2 + 12Q_b + 4\times10^{-4}Q_b^2 + 0.03T_{db} - 3\times10^{-4}T_{db}^2 \\ -0.38 - 2.8Q_b - 0.001Q_b^2 - 0.02T_{db} + 18\times10^{-5}T_{db}^2 \\ -7.9 + 0.5Q_b - 3\times10^{-5}Q_b^2 + 0.6T_{db} - 6\times10^{-3}T_{db}^2 \end{bmatrix}. \tag{31}$$

For a suitable value of $\beta$, the next point is determined as:

$$X_1 = X_0 + \beta U_0. \tag{32}$$

The optimal descent in the direction of $U_0$ is then calculated as:

$$f(X_1) = F(\beta). \tag{33}$$

The optimisation algorithm generates the next point by using the iteration procedure according to the flowchart shown in Fig. 2. The values corresponding to each new point are then fed to the estimated objective function to predict the system response and the overall power consumption. A termination criterion for the optimizer algorithm is proposed by comparing the projection values of the gradient vector. To terminate the algorithm for each hour in the vicinity of the optimum, $U(X)$=0, the current value of the gradient projection is chosen to be less than 0.005 in magnitude. The optimal control settings are then generated for the real-world process. Next, the algorithm starts for the following operational hour. The total energy usage for each summer day can be obtained by summation of the system energy consumption in each working hour. The remainder of this section discusses the effects of the proposed control strategy on the cooling system performance in terms of sensitivity, energy and thermal comfort.

### 5.1 Sensitivity Analysis

Sensitivity analysis is conducted to determine which optimal set-points have a significant effect on the power consumption of each component. Variations of the controlled variables with respect to other effective variables for each component are studied in order to investigate the influence of each controlled variable on the system performance. As depicted in Fig. 4(a), both the cooling load and chilled water temperature have a significant effect on the optimal refrigerant mass flow rate. Further increasing either one of the variables will increase the optimal refrigerant flow rate. Fig. 4(b) shows that the optimal supply air temperature is more sensitive to variations of the building's cooling load than to changes in the refrigerant flow rate. In addition, the optimal value of the supply air temperature decreases with an increase of both the building's cooling load and chilled water temperature. Moreover, Fig. 4(b) illustrates that the optimal supply air temperature should be lowered while the refrigerant flow value should be increased with a larger value of the cooling load. Nevertheless, the results show that changes in the supply air temperature do not have a considerable effect on the condenser fan power.

A high sensitivity to the building's cooling load is attributed to the increasing overall power usage in the sense that a cooling load's sensitivity above unity implies an increase more than 1% in the total power consumption for every increase of $Q_b$ by 1%. This high sensitivity suggests that for high cooling load conditions, any addition to the cooling demand should be realised by structural design changes of the chilled water loop system in the form of parallel piping rather than by simply decreasing the chilled water supply temperature $T_{chw,o}$ with the existing pipes. The ambient dry-bulb temperature has a high impact on the performance of the air-cooled condenser and its power consumption. This is because the dry-bulb temperature affects directly the required mass flow rate of the condenser.

### 5.2 Energy Analysis

The optimal set-points obtained from the proposed gradient projection algorithm are then fed to TRANSYS in order to compute the energy usage of the system components. These set-points of the controlled variables are aimed to minimize the total power consumption of the cooling plant while fulfilling the cooling demand of the building. The energy savings potential for the mentioned cooling plant is shown in Fig. 5. It can be seen that the average power consumed under the calculated optimal set-points values is nearly 11.4% less than under the commonly-used controls. Power consumption values of the chiller compressor and air-cooled condenser with optimization are less than those without optimization while the supply fan power usage is higher than that without optimization. The energy savings potential of the proposed approach for the compressor and condenser fan are respectively 8.8% and 4.6% while the supply fan power consumption increases by 2.3%. The reason is that a higher chilled water temperature requires less heat transfer in the evaporator and causes a lower refrigerant superheat temperature leaving the evaporator. Therefore, the compressor should work at a lower pressure, and in turn, reduce its power consumption. When the refrigerant mass flow rate decreases as a result of the increased chilled water temperature, the power consumption of the air-cooled condenser fan also reduces because a lower condensing pressure causes less power usage in the condenser fan. Meanwhile, as the chilled water temperature increases, the heat transfer efficiency of the ducted fan-coil unit becomes lower. Therefore, more supply air will be required to compensate for the efficiency drop, which slightly increases the power consumption of the supply fan. In contrast, a lower chilled water temperature can save the power consumption of the supply fan, but it deteriorates the chiller's coefficient of performance, resulting in more consumption of its power. In addition, the results obtained show a relatively high influence of the ambient dry-bulb temperature on the performance of the condenser fan. Fig. 6 shows the control functions over ranges of the system's power consumption. It is obvious that the values of the chilled water and supply air temperature with optimization are higher than those without optimization while the optimized refrigerant mass flow rate is less than the refrigerant flow rate without optimization. From this discussion, the proposed optimal control strategy for the overall cooling plant results in control settings for higher energy-efficiency via minimizing the power consumption of the entire system. Besides, it should be noted that the gradient projection method used in this paper can converge to at least a local minimum regardless of the convexity characteristics of the objective function and constraints. The proposed method is rather computationally-effective for on-line application.

## 5.3 Thermal Comfort

For investigation of the influence of the optimization approach on the building thermal comfort, most widely used is a thermal comfort index, called the predicted mean vote (PMV). The PMV model predicts the mean thermal sensation vote on a standard scale of thermal feelings for a large group of people in a given indoor space. The values of the PMV index range from -3 to +3, corresponding to the occupant's feelings from cold to hot, while its null value means neutral. The PMV-based thermal comfort can be achieved with low power consumption by appropriately determining the indoor-air condition via a combination of temperature, humidity and velocity of the indoor air [26]. The PMV values between -1 and 1 are in the range that 75% people are favourable while between -0.5 and 0.5 implies satisfaction of up to 90%. The hourly average PMV for summer months is shown in Fig. 7. The results show that all PMV responses lie in the acceptable range, i.e. $-1 < \text{PMV} < +1$. Furthermore, results show that the minimum, maximum and average values of the indoor temperature after optimization are respectively 21.6°C, 26.8°C and 24.6°C, corresponding respectively to the indoor relative humidity 43%, 58% and 53%. Thus, both the indoor temperature and humidity are found in the comfort range.

# 6. Conclusion

In this paper, we have addressed the modelling and optimization problem of a central cooling plant to target energy savings and verified the proposed approach in an office building. A gradient projection-based optimization-simulation algorithm is developed to find the optimizing set-points of the supply chilled water temperature, refrigerant flow rate and supply air temperature. A real-world building, located in a hot and dry climate region, together with its existing central cooling plant is used for experimentation and data collection. By using the monitored data, mathematical models for the set-up components are developed and implemented in a transient simulation program in order to predict the performance of the integrated system operating in various conditions. Simulation-experimental results showed that by applying this approach, an air-cooled central cooling plant

HVAC system can achieve significant improvements in energy-efficiency and performance, especially in part-load conditions.

## Acknowledgement

This work is supported, in part, by The New South Wales Government through its Environmental Trust, Project 2012/RDS/034.

## References

[1] F.W. Yu , K.T. Chan, Energy signatures for assessing the energy performance of chillers, Energy and Buildings 37 (7) (2005) 739-746.

[2] Y.C. Chang, F.A. Lin, C.H. Lin, Optimal chiller sequencing by branch and bound method for saving energy, Energy Conversion and Management 46 (13-14) (2005) 2158-2172.

[3] Z. Xiaosong, X. Guoying, K.T. Chan, X. Yi, A novel energy-saving method for air-cooled chiller plant by parallel connection, Applied Thermal Engineering 26 (16) (2006), 2012-2019.

[4] L. Cecchinato, Part load efficiency of packaged air-cooled water chillers with inverter driven scroll compressors, Energy Conversion and Management 51 (7) (2010) 1500-1509.

[5] G. Huang, Y. Sun, P. Li, Fusion of redundant measurements for enhancing the reliability of total cooling load based chiller sequencing control, Automation in Construction 20 (7) (2011) 789-798.

[6] Q. Wang, Y.Q. Liu, G.F. Liang, J.R. Li, S.F. Sun, G.M. Chen, Development and experimental validation of a novel indirect-expansion solar-assisted multifunctional heat pump, Energy and Buildings 43 (2011) 300-304.

[7] A. Al-Alili, Y. Hwang, R. Radermacher, I. Kubo, A high efficiency solar air conditioner using concentrating photovoltaic/thermal collectors, Applied Energy 93 (2012), 138-147.

[8] Q.P. Ha, V. Vakiloroaya, A novel solar-assisted air-conditioner system for energy savings with performance enhancement, Procedia Engineering 49 (2012), 116-123.

[9] V. Congradac, F. Kulic, HVAC system optimisation with $CO_2$ concentration control using genetic algorithms, Energy and Buildings 41 (5) (2009) 571-577.

[10] A.P. Wemhoff, Application of optimisation techniques on lumped HVAC models for energy conservation, Energy and Buildings 42 (12) (2010) 2445-2451.

[11] M. Zaheeruddin, M. Ning, Neuro-optimal operation of a variable air volume HVAC&R system, Applied Thermal Engineering 30 (5) (2010) 385-399.

[12] Z. Ma, S. Wang, Supervisory and optimal control of central chiller plants using simplified adaptive models and genetic algorithm, Applied Energy, 88 (1) (2011) 198-211.

[13] A. Beghi, L. Cecchinato, Modelling and adaptive control of small capacity chillers for HVAC applications, Applied Thermal Engineering, 31 (6-7) (2011) 1125-1134.

[14] TRNSYS software. A transient system simulation program, version 16. Wisconsis-Madison University. Available: <http://sell.me.wisc.edu/trnsys/>.

[15] V. Vakiloroaya, M. Khatibi, Q. P. Ha, B. Samali, "New Integrated Hybrid Evaporative Cooling System for HVAC Energy Efficiency Improvement," Proceedings of the 2011 IEEE/SICE International Symposium on System Integration, Kyoto, Japan, 2011, pp. 772-778.

[16] D.J. Swider, A comparison of empirically based steady-state models for vapour compression liquid chillers, Applied Thermal Engineering 23 (5) (2003) 539-556.

[17] T.S. Lee, W.C. Lu, An evaluation of empirically-based models for predicting energy performance of vapour-compression chillers, Applied Energy 87 (11) (2010) 3486-3493.

[18] D. Monfet, R. Zmeureanu, Ongoing commissioning of water-cooled electric chillers using benchmarking models, Applied Energy 92 (2012) 99-108.

[19] V. Vakiloroaya, J.G. Zhu, Q.P. Ha, Modelling and optimisation of direct expansion air conditioning system for commercial building energy saving, Proceedings of the 28th International Symposium on Automation and Robotics in Construction (ISARC 2011), Seoul, Korea, 2011, pp. 198-202.

[20] X. Zhifang, S. Lin, O. Hongfei, Refrigeration Flow Characteristics of Electronic Expansion Valve Based on Thermodynamic Analysis and Experiment, Applied Thermal Engineering 28 (2-3) (2008) 238-243.

[21] S.C. Sekhar, L.T. Tan, Optimization of cooling coil performance during operation stages for improved humidity control, Energy and Buildings 41 (2) (2009) 229-233.

[22] G.Y. Jin, W.J. Cai, Y.W. Wang, Y. Yao, A simple dynamic model of cooling coil unit, Energy Conversion and Management 47 (15-16) (2006) 2659-2672.

[23] J.A. Snyman, Practical mathematical optimization: An introduction to basic optimization theory and classical and new gradient-based algorithms, Springer Inc, USA, 2005.

[24] ANSI/ASHRAE Standard 140, Standard Method of Test for the Evaluation of Building Energy Analysis Computer Program, American Society of Heating, Refrigerating and Air-Conditioning, 2007.

[25] Minitab Inc, Minitab User's Guide Release 16, 2010.

[26] S. Atthajariyakul, T. Leephakpreeda, Real-time determination of optimal indoor-air condition for thermal comfort, air quality and efficient energy usage. Energy and Buildings, 36 (7) (2004) 720-733.

## Figure Captions

Fig. 1. Diagrams: (a) schematic diagram of the central cooling plant, (b) p-h diagram of the air-cooled chiller

Fig. 2. Optimization algorithm flowchart

Fig. 3. Comparison of measured and simulated compressor power

Fig. 4. Optimal controlled variables: (a) refrigerant mass flow rate versus chilled water temperature and building cooling load, (b) supply air temperature versus refrigerant mass flow rate and building cooling load

Fig. 5. Air-cooled cooling plant power consumption

Fig. 6. Control functions over the system power consumption range

Fig. 7. PMV values for the optimized cooling plant

## Table Captions

Table 1. Corresponding coefficients of the models and constraint

Table 2. Main parameters used for simulation

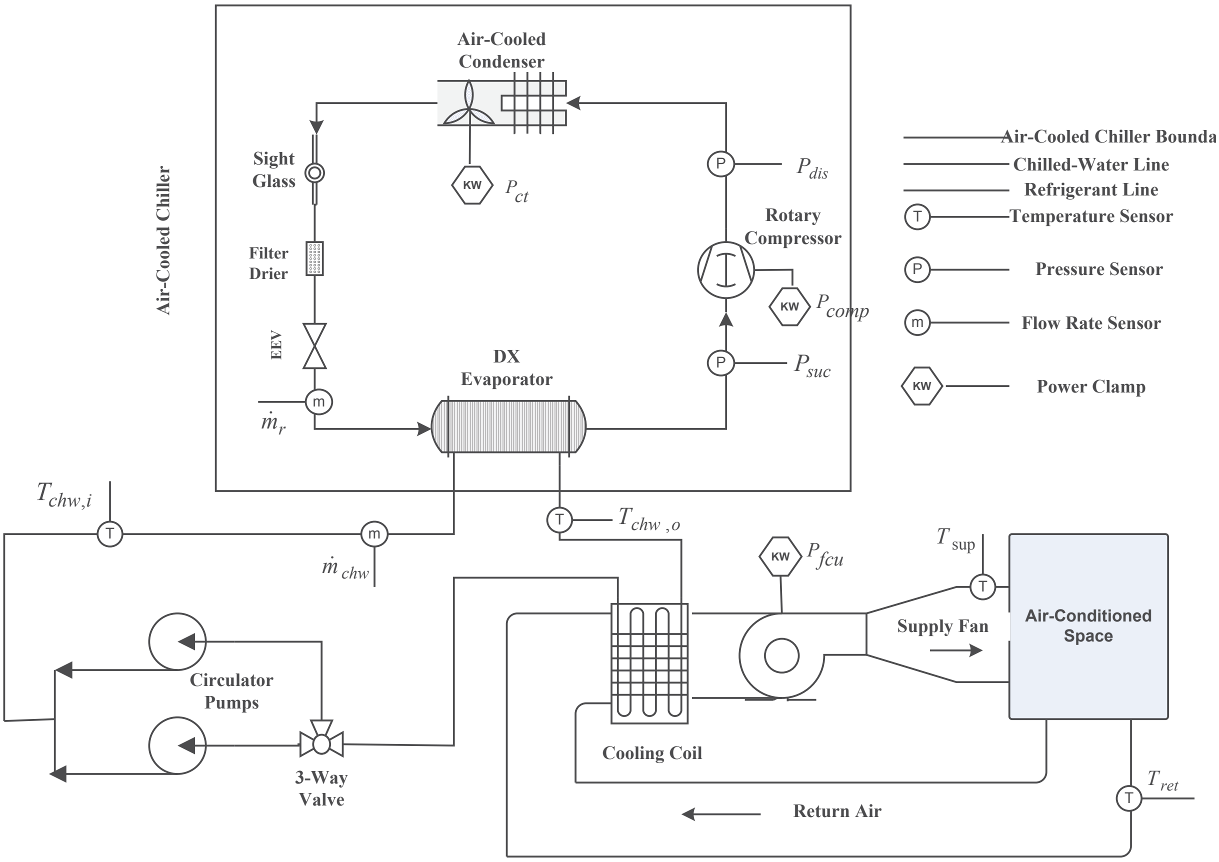


(a)

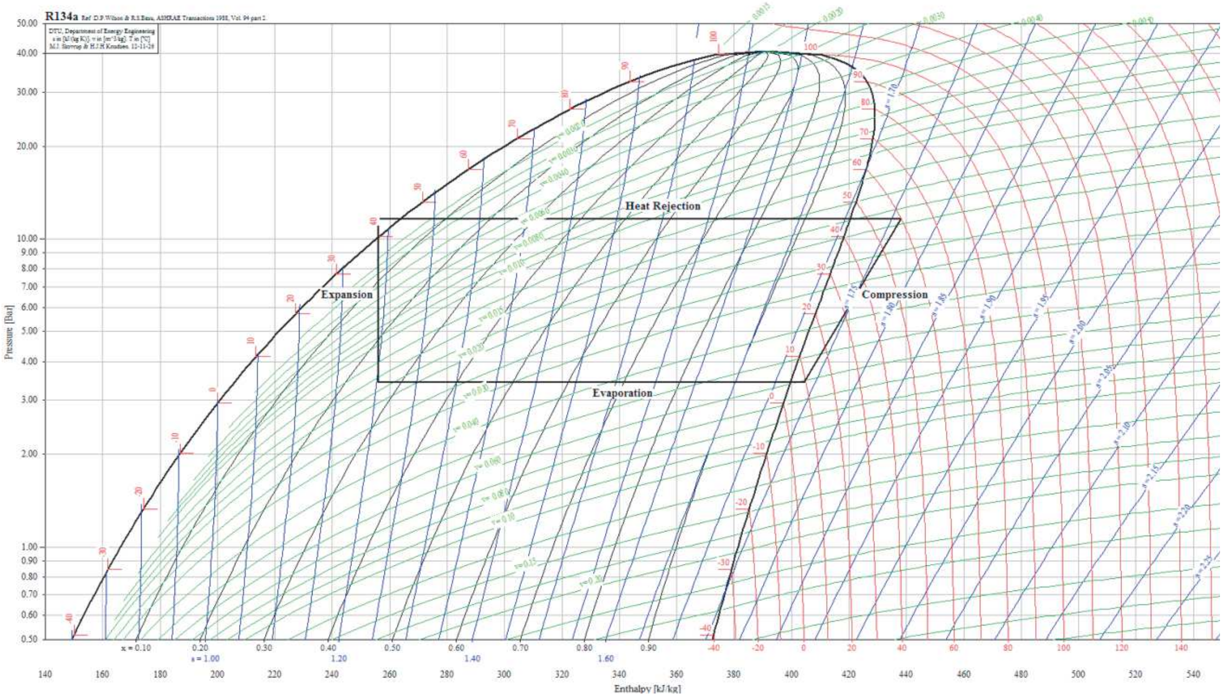


(b)

Fig. 1. Diagrams: (a) schematic of the central cooling plant (b) p-h diagram of the air-cooled chiller.

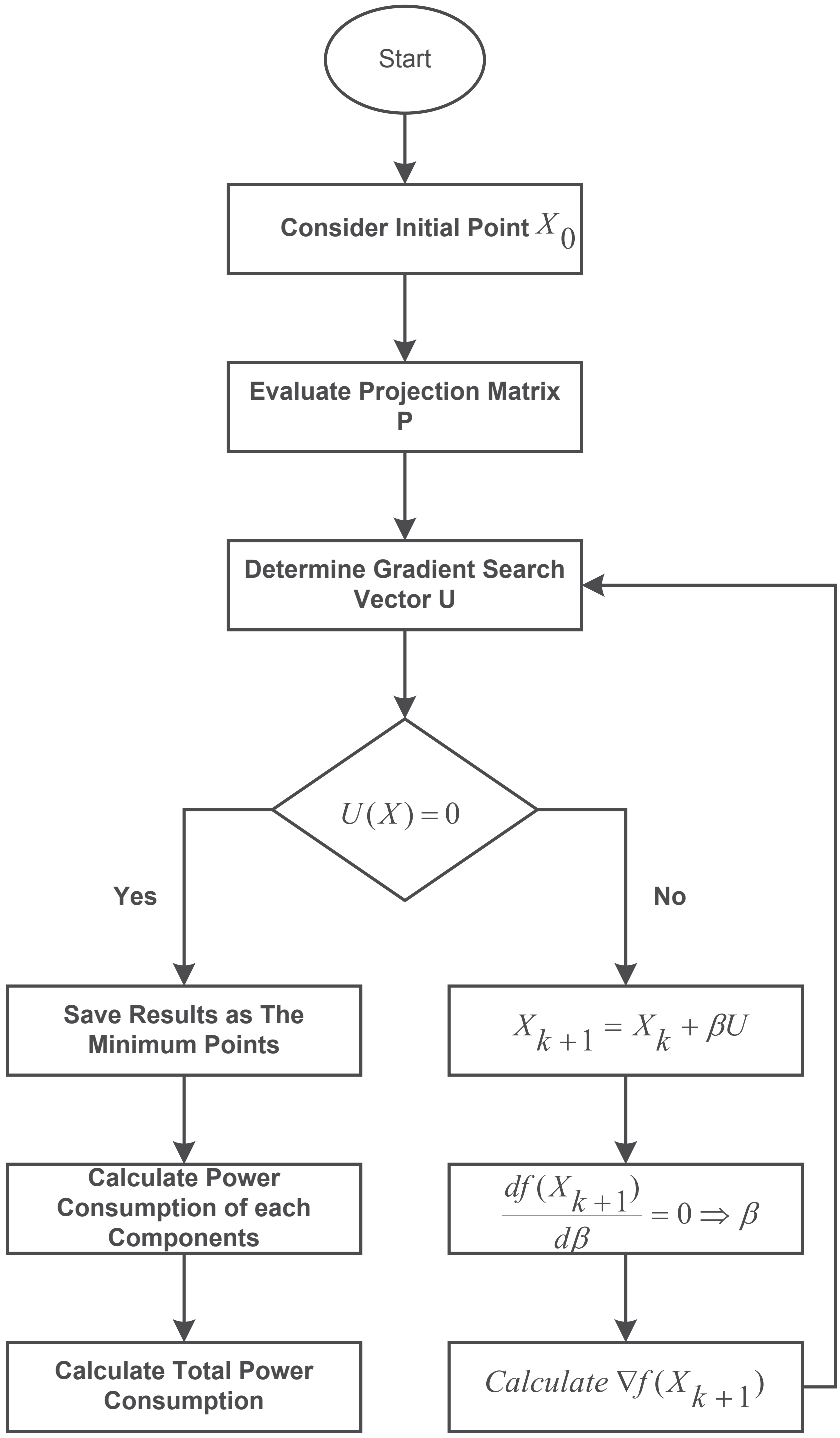


Fig. 2. Optimization algorithm flowchart

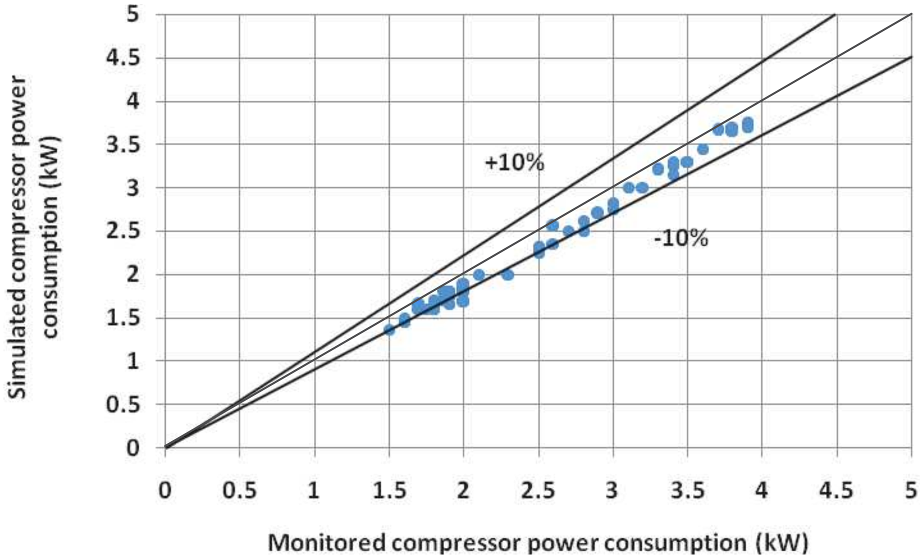


Fig. 3. Comparison of measured and simulated compressor power

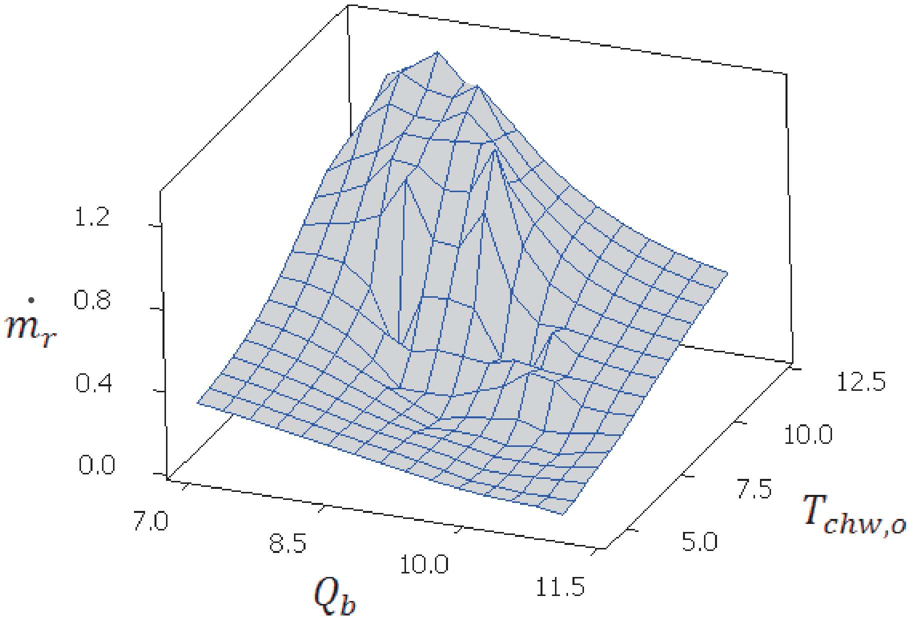


(a)

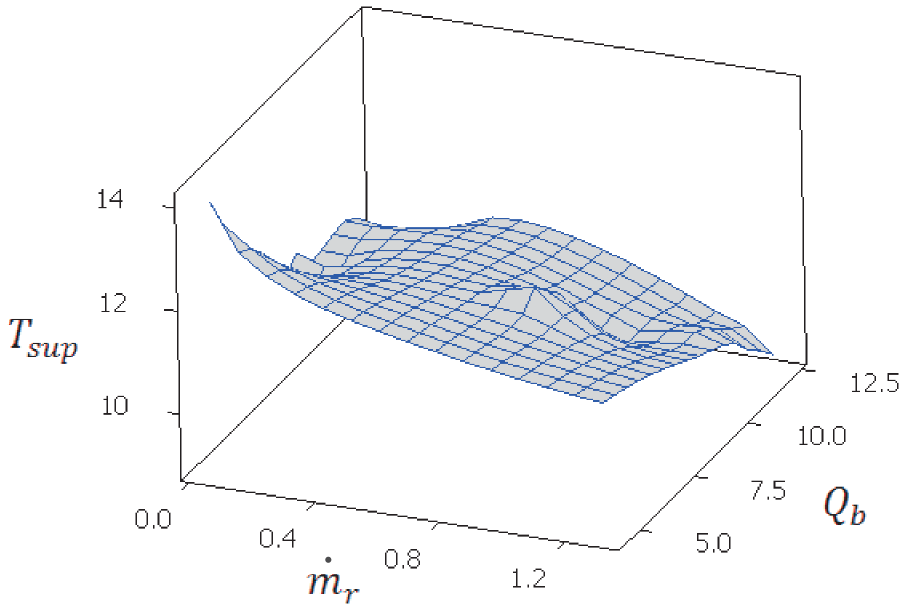


(b)

Fig. 4. Optimal controlled variables: (a) refrigerant mass flow rate versus chilled water temperature and building cooling load, (b) supply air temperature versus refrigerant mass flow rate and building cooling load

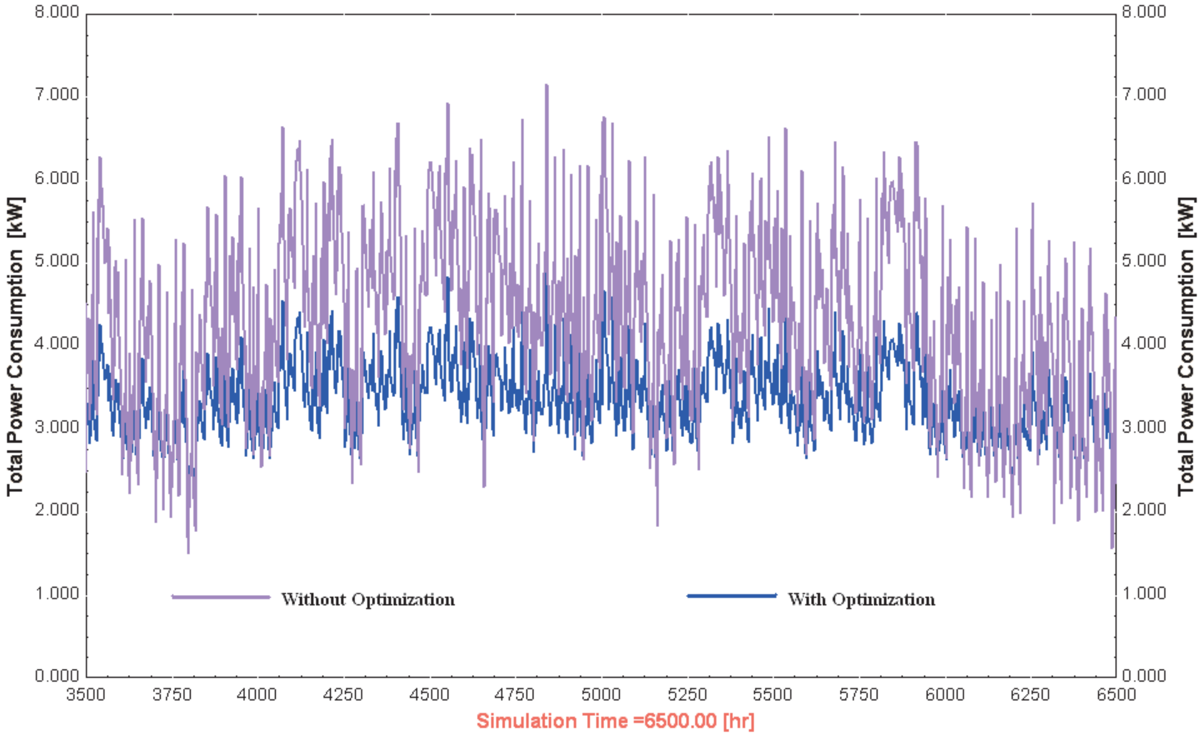


Fig. 5. Air-cooled cooling plant power consumption

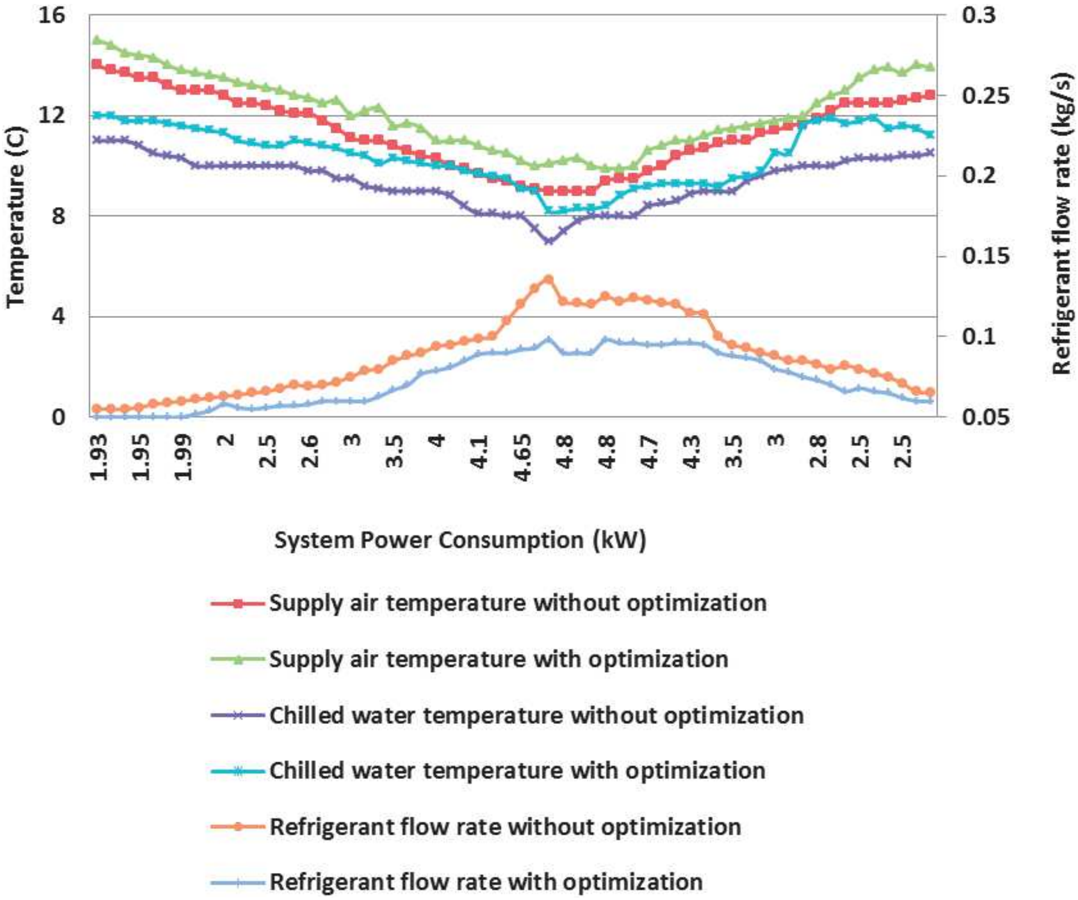


Fig. 6. Control functions over the system power consumption range

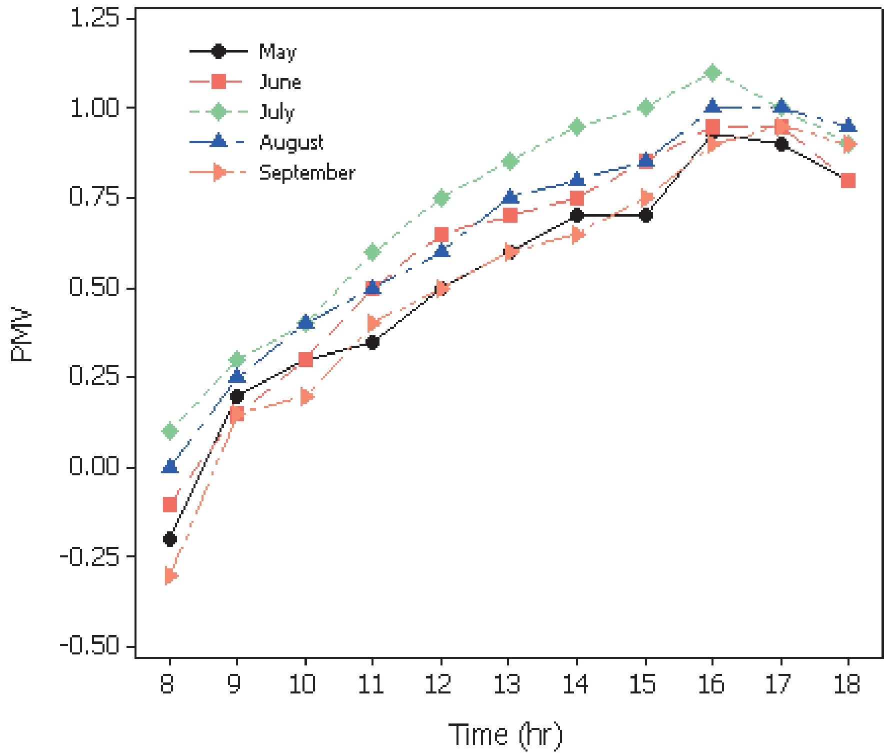


Fig. 7. PMV values for the optimized cooling plant

| Equation | Coefficients |
|---|---|
| (2) | $a_0 = 0.038$ $a_1 = -0.8$ $a_2 = 1.324$ $a_3 = -0.745$ $a_4 = 0.002$ |
| (8) | $b_0 = -2.468$ $b_1 = -0.49$ $b_2 = 0.055$ $b_3 = 0.363$ $b_4 = -0.57$<br>$b_5 = -0.24$ $b_6 = 0.044$ $b_7 = -0.01$ $b_8 = 0.021$ $b_9 = 0.152$ |
| (12) | $a_5 = 0.063$ $a_6 = -0.5$ $a_7 = 0.021$ $a_8 = -0.8$ $a_9 = 0.003$ |
| (14) | $c_0 = 0.474$ $c_1 = -14.141$ $c_2 = 3.30$ $c_3 = 0.622$ $c_4 = -0.092$ $c_5 = -0.006$ |
| (17) | $d_0 = 7.215$ $d_1 = -1.711$ $d_2 = 0.07$ $d_3 = 0.031$ $d_4 = 0.110$<br>$d_5 = -0.001$ $d_6 = 0.040$ $d_7 = -0.01$ $d_8 = -0.002$ $d_9 = -0.032$ |
| (35) | $e_0 = -4.37$ $e_1 = 1$ $e_2 = -0.054$ $e_3 = 0.071$ $e_4 = 0.02$ $e_5 = 0.028$ |

Table 1. Corresponding coefficients of the models and constraint

| | |
|---|---|
| Air-cooled chiller nominal cooling capacity (kW) | 17.5 |
| Refrigerant type | R134a |
| Design evaporative temperature (°C) | 4.4 |
| Design chilled water temperature (°C) | 7 |
| Design chilled water mass flow rate ($m^3$/h) | 1.8 |
| Rated electric power of chilled-water pump (kW) | 0.2 |
| Design condensing temperature (°C) | 45 |
| Design suction pressure (kPa) | 342 |
| Design discharge pressure (kPa) | 1160 |
| Total efficiency of the compressor | 0.8 |
| Design refrigerant mass flow rate (kg/s) | 0.115 |
| Ducted fan-coil unit supply air flow rate ($m^3$/h) | 3400 |
| Rated electric power of VAV fan (kW) | 1.2 |
| Cooling coil tube material | copper |
| Cooling coil fin material | aluminum |
| Cooling coil outer diameter of tubes (mm) | 16 |
| Cooling coil wall thickness of tubes (mm) | 0.5 |
| Cooling coil number of rows | 4 |
| Cooling coil number of fins | 650 |
| Cooling coil face area ($m^2$) | 0.4 |
| Cooling coil longitudinal space of tubes (cm) | 3.17 |
| Cooling coil transverse space of tubes (cm) | 3.8 |

Table 2. Main parameters used for simulation